Pushing nanoparticles with light — A femtonewton resolved measurement of optical scattering forces

C. Zensen' , N. Villadsen' , F. Winterer, S. R. Keiding, and T. Lohmüller'

Citation: APL Photonics **1**, 026102 (2016); doi: 10.1063/1.4945351

View online: http://dx.doi.org/10.1063/1.4945351

View Table of Contents: http://aip.scitation.org/toc/app/1/2

Published by the American Institute of Physics

APL PHOTONICS **1**, 026102 (2016)

Pushing nanoparticles with light — A femtonewton resolved measurement of optical scattering forces

C. Zensen,[1,2,a] N. Villadsen,[3,a] F. Winterer,[1] S. R. Keiding,[3] and T. Lohmüller[1,2,b]

[1]*Photonics and Optoelectronics Group, Department of Physics and Center for Nanoscience (CeNS), Ludwig-Maximilians-Universität München, 80799 Munich, Germany*
[2]*Nanosystems Initiative Munich, Schellingstraße 4, 80799 München, Germany*
[3]*Department of Chemistry, Aarhus University, DK 8000 Aarhus C, Denmark*

(Received 14 December 2015; accepted 24 February 2016; published online 9 May 2016)

Optomechanical manipulation of plasmonic nanoparticles is an area of current interest, both fundamental and applied. However, no experimental method is available to determine the forward-directed scattering force that dominates for incident light of a wavelength close to the plasmon resonance. Here, we demonstrate how the scattering force acting on a single gold nanoparticle in solution can be measured. An optically trapped 80 nm particle was repetitively pushed from the side with laser light resonant to the particle plasmon frequency. A lock-in analysis of the particle movement provides a measured value for the scattering force. We obtain a resolution of less than 3 femtonewtons which is an order of magnitude smaller than any measurement of switchable forces performed on nanoparticles in solution with single beam optical tweezers to date. We compared the results of the force measurement with Mie simulations of the optical scattering force on a gold nanoparticle and found good agreement between experiment and theory within a few fN. [http://dx.doi.org/10.1063/1.4945351]

The coupling of optical and mechanical degrees of freedom is the underlying tool for many investigations of small forces in the micro- and nanometer range. Applications range from the ability to cool down atoms and ions in atomic physics,[1] gravitational wave interferometry in cavity optomechanics,[2] and single-molecule force spectroscopy in biophysics.[3,4] Each of these techniques corresponds to a characteristic length scale. On the subnanometer scale and the micronscale, optomechanical manipulation is already an established technique that enables precise force determination, whereas on the nanometer scale, quantitative force measurements are not as well explored.[5] As pointed out by recent reviews[6,7] optical manipulation of nanometer metal particles has attracted a lot of interest in fields where nanometer displacements and femtonewton forces apply, such as nanofabrication[8] or cellular biophysics.[3,9] The plasmonic nature of metal nanoparticles results in a significantly enhanced and strongly wavelength dependent mechanical response on incident light in the visible regime.[10–12] Consequently, gold nanoparticles have been shown to be a good choice for sensitive force detection.[13]

The optical force can be decomposed into two contributions:[14] the scattering force, and the gradient force. The scattering force represents the momentum transfer from the external radiation field to the nanoparticle by scattering and absorption[6,15] and is pointing along the axis of the energy flux of the light beam. Whereas, the gradient force is directed along the intensity gradient of the beam. If the gradient force exceeds the scattering force, particles can be trapped by light.[16] While

[a]C. Zensen and N. Villadsen contributed equally to this work.
[b]Electronic mail: t.lohmueller@lmu.de

scattering forces have been considered theoretically for decades[17] and the emergent field of photonic force microscopy builds on measuring net forces on nanoparticles in solution,[5] to our knowledge isolated scattering forces on a single gold nanoparticle have never been determined experimentally. However, measuring scattering forces is challenging due to the inherent thermal fluctuations of the nanoparticles caused by the surrounding liquid. The application of strong laser light close to the plasmon resonance resulting in strong scattering forces goes along with substantial heating. Low scattering forces, on the other hand, are hidden by the inherent thermal fluctuations of the particle.

In this article we have overcome both the challenge of the force sensitivity and the low scattering force by applying a periodic scattering force to a trapped gold nanoparticle. More precisely the resonant femtonewton scattering forces on single gold nanoparticles were measured in a non-resonant single beam optical tweezer with dark field detection.[18] We introduce a "switchable" optical scattering force by coupling a resonant laser through a single-mode fiber perpendicular to the trapping beam. The switching process (on/off) is controlled by blocking the laser output in intervals with a chopper wheel. By applying a post-elimination technique[19,20] for thermal noise based on a lock-in strategy, a force sensitivity of 2.4 fN is obtained. This value is lower than the force sensitivity obtained before in the context of optical tweezers applications in liquids.[5,21–23] For measurements of switchable forces with conventional optical tweezers, this sensitivity is even an improvement of an order of magnitude[24] and thus permits the determination of the scattering force on a plasmonic nanoparticle. A comparison with theoretical calculations of the scattering force based on Mie scattering theory shows good agreement.

In the experiments shown here, the optical scattering force on a single gold nanoparticle is measured by applying it as a perturbation of the fluctuative motion of a particle in the harmonic potential of the laser trap (Figure 1). For the detection and measurement of femtonewton scattering forces on single gold nanoparticles, a single beam optical tweezer setup was used. The measurement was achieved by trapping single gold nanoparticles (Nanopartz, Accurate™ Spherical Gold Nanoparticles, A11-80) with a diameter of 80 nm in a nonresonant 1064 nm CW laser (Cobolt AB, Cobolt Rumba™, 05-01 Series). The laser was coupled into an upright microscope (ZEISS, Axiovert) and focused through a water immersion objective (ZEISS, 100×, NA = 1.0). For 80 nm gold nanoparticles that were used throughout this work, a trapping laser power of 50 mW (measured after the objective) resulted in a trap stiffness of 2.6 fN/nm. For these conditions, stable optical trapping of a single gold nanoparticle was possible over tens of minutes. Throughout all experiments, several control measurements were performed to ensure that indeed only one single gold nanoparticle was trapped at the time by the laser beam (for details, please see supplementary material:[25] "Optical trapping of single particles"). Trapping took place in water with a temperature of 24 °C, however, laser irradiation would lead to an increase of the particle temperature to 50 °C.[25] Inside an optical trap, however, fluctuations of the heated particle or "hot Brownian motion"[26] needs to be taken into account, which results in an effective particle temperature of only 35 °C.

The use of a dark field oil condenser (ZEISS, NA = 1.2/1.4) and white light illumination allowed for video detecting of the subwavelength gold nanoparticle because of the large scattering cross section in the visible wavelength regime.[18] Due to scattering forces of the tweezing laser present also for off-resonant laser wavelengths gold nanoparticles are trapped slightly below the

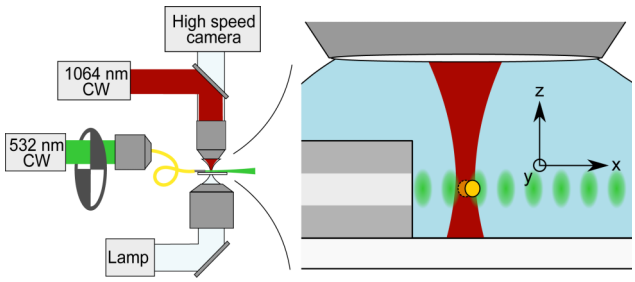

FIG. 1. Schematic sketch of the microscopy setup for femtonewton precise measurement of scattering forces. A gold nanoparticle is trapped in water with a focused near infrared laser, while chopped green laser light from a fiber pushes the particle orthogonal to the trapping beam.

focus of the trapping laser. Consequently, the tweezer was prefocused with a lens and a beam expander in order to move the particle into the focus of the camera and improve the image quality. Videos were recorded with a high speed camera (PCO AG, pco.dimax HD) at an image acquisition speed of 500 Hz and an exposure time of 1.9 ms. A notch filter for both laser wavelengths (532 and 1064 nm) was positioned in the imaging path to avoid artifacts of the chopping. Position tracking of the acquired image sequences was done using a Matlab algorithm published by Parthasarathy.[27]

A chopper wheel (Newport, New Focus Optical Chopper 3501) was placed in the 532 nm CW laser beam (Coherent, Verdi 10), which is resonant with the plasmon frequency of the nanoparticle. The rotational frequency of the chopper wheel was synchronized with the image acquisition frequency using a home built frequency splitter. In a typical experiment, 2^{11} chopper cycles with a frequency of 31.25 Hz or one sixteenth of the image acquisition frequency were considered. The 532 nm laser was coupled through an optical single-mode fiber (Thorlabs, P1-460B-FC-2, NA = 0.10-0.14). The output end of the fiber was stripped down to the 125 μm cladding diameter and placed on the microscope cover slide, with the fiber output propagating in the x-axis. With this, the 532 nm laser beam is perpendicular to the trapping laser beam, which propagates in the $-z$-axis. The relative position of the trapped nanoparticle and the fiber was controlled using a piezocontroller (LINOS, PiezoController CU30). The fiber end was positioned 75 μm away from the trapped particle in the x-axis. The beam diverges slightly coming out of the fiber. Therefore we used a CCD camera (Thorlabs) for beam profiling, and determined the beam width at the particle to be 6 ± 2 μm corrected for the refractive index of water. Since the diameter of the gold nanoparticle (80 nm) was much smaller than this beam width, a spatial intensity gradient can be neglected. Irradiation with laser light at the plasmon resonance frequency therefore results only in a forward-directed scattering force. The power density of the resonant laser was chosen so low that heating effects do not play a role here. This was confirmed by control measurements for the particle position distribution with the green laser on and off showing that this difference in temperature cannot be resolved.

It is also important that the possibility of a thermophoresis that would push the particle along a temperature gradient due to plasmonic heating[28] can be neglected for our experimental conditions. A gold nanoparticle is in thermal equilibrium within picoseconds after the irradiation with a laser beam due to the high thermal conductivity of gold.[29,30] Throughout our measurements, the exposure time of the optically trapped gold particles was in the range of several milliseconds. Although the particles are only irradiated from one side, the particle temperature is therefore completely uniform.[31]

The particle trapped in water can be described by the Langevin equation,[32] for simplicity only the x-direction is considered. The equation is extended with the chopper controlled scattering force $F_S(t)$,[19]

$$m\ddot{x}(t) + \kappa x(t) + \gamma \dot{x}(t) = \xi(t) + F_S(t), \tag{1}$$

where m is the mass of the particle, κ is the harmonic force constant of the optical trap, $\xi(t)$ is the stochastic Brownian force, and $\gamma = 6\pi r\eta$ is the drag coefficient, with r being the radius of the particle and η the viscosity of the fluid. In the present case, the dynamics of the scattering force can be modelled by the Heaviside step function, H,

$$F_S(t) = F_S \cdot \sum_{0}^{k=N-1} \left[H(t - kt_p) - H(t - kt_p - \frac{t_p}{2}) \right], \tag{2}$$

where F_S is the magnitude of the applied scattering force, $N = \frac{t_m}{t_p}$ is the number of repetitions of force steps, t_m is the total measurement time, and t_p the period of the force step.

Applying the step force results in a displacement of the particle. However, due to Brownian motion, a single push cannot be distinguished from the thermal fluctuations, because the position standard deviation is larger than the displacement caused by a single step. Figure 2(a) shows the collective displacement of two periods of pushing and the thermal fluctuations, with no visible sign of the switching of the scattering force. For the present experimental configuration based on the periodic repetition of a mechanical stimulus, it is possible to bypass the Brownian noise.[20] By averaging the tracked time series with respect to the chopping period, the spatial displacement is revealed with subpixel resolution. In Figure 2(b), the two cycles of Figure 2(a) have been averaged

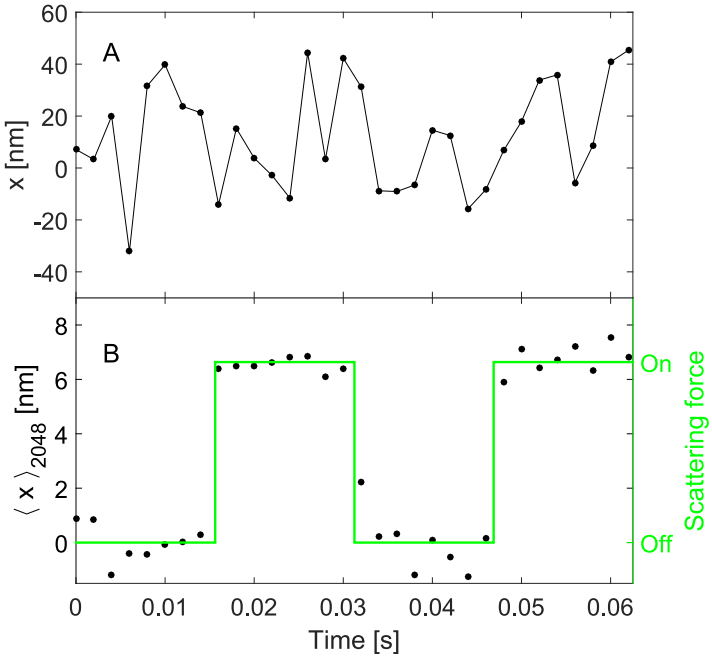

FIG. 2. (a) Raw trace of a trapped particle, showing the first two pushing cycles, though the displacement from the scattering force is hidden by thermal fluctuations. (b) The averaged trace of 2^{11} repetitions, clearly showing the displacement resulting from switching the optical scattering force "on" and "off" for intervals of 16 ms. The complete measurement was performed for a duration of 65.54 s.

with all the following events. From the resulting trace a maximal displacement of 6.6 nm is revealed if the maximal scattering force is applied.

Analysis of particle movements in optical tweezers can be done using power spectral densities.[33] Here the method is used first to calibrate the tweezer and subsequently for an accurate analytical determination of the scattering force. Fourier-transforming Eq. (1) with Eq. (2) inserted provides an analytical solution of the differential equation. Hence, similar to the argumentation given in Ref. 19, we derived an expression for the expectation value of the power spectral density (see supplementary material[25])

$$\langle S_x(f)\rangle = \frac{1}{(2\pi\gamma)^2}\frac{1}{f_c^2+f^2}\left(2\gamma k_B T + \frac{F_S^2}{8\pi^2 f^2 \cdot t_m}\cdot\left(\frac{\sin\pi f t_m}{\cos\frac{\pi}{2} f t_p}\right)^2\right), \tag{3}$$

where $f_c = \frac{\kappa}{2\pi\gamma}$ is the corner frequency. In this form, the first term of the sum can be recognized as the diffusive part whereas the second summand is the result of the periodically pushing scattering force $F_S(t)$. At low frequencies ($f \ll f_c$) and without the scattering force, the power spectrum is independent on frequency

$$S_0 = \frac{2\pi\gamma k_B T}{\kappa^2}. \tag{4}$$

Though, the plateau does depend on the force constant. It is thus possible to measure the trap stiffness even though the time resolution of the detection is below the corner frequency. The periodical scattering force only influences the power spectral density at the chopping frequency and uneven higher harmonics of the chopping frequency. Using a measurement time of $t_m = 2^k t_p$, where k is an integer, the resulting peak power at the chopping frequency is

$$\langle S_x(f_{ch})\rangle = \frac{1}{8\pi^4\gamma^2}\frac{t_m}{(f_c^2+t_p^{-2})}F_S^2. \tag{5}$$

Using Equations (4) and (5), the radius and viscosity are included through the drag coefficient. Consequently they both influence the uncertainty of the scattering force determination (for details please

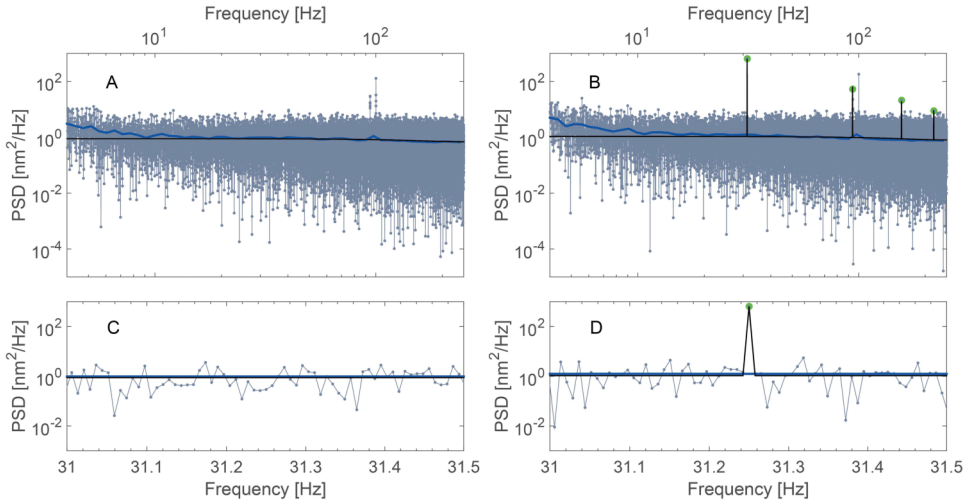

FIG. 3. (a) Power spectral density plot of the movement of a trapped gold nanoparticle. The black line is a fit providing a force constant $\kappa = 2.4$ fN/nm. The blue line is an average of logarithmic windows. The measurement time was 65.54 s using 500 fps, resulting in a frequency sampling of 15.4 mHz. The height of the peaks can be determined with a precision of less than 1 nm^2/Hz. (b) Power spectral density plot of the movement of a trapped gold nanoparticle measured as in (a) but in presence of a chopped scattering beam (532 nm, 31.25 Hz chopper frequency). The large green dots highlight the measured power spectral density at the chopping frequency and the higher harmonics. The black line is now a plot of the analytic conversion from the peak height of the first harmonic to a corresponding value of the scattering force of 23 fN. (c) and (d) are zoom of (a) and (b). Note that the first noise peak in (a) does not overlap the third harmonic of the chopping frequency.

see supplementary material,[25] section "Maximum error calculation"). The issue of motion blurring and aliasing of both the calibration analysis and scattering force analysis, due to the finite recording exposure time and frame rate is addressed using the corrections and fitting methods described in the papers of Wong and Halvorsen[34] and Berg-Sørensen and Flyvbjerg.[33]

The system was calibrated based on traces of the trapped particle without the scattering beam. Figure 3(a) is a typical example of a power spectral density plot of such a trace. The log-space average (blue line) on top of the measured power spectral density (blue datapoints) serves as a guide to the eye for the overall frequency dependence. The black line is a fit to the measured power spectral density above 20 Hz as described in the paper of Berg-Sørensen and Flyvbjerg[33] and taking aliasing and blur into account. The fit including the temperature of 35 °C and the associated viscosity $\eta = 0.7191$ mPa s according to[35] gave a force constant of $\kappa = 2.6$ fN/nm. The equivalent corner frequency is $f_c = 603$ Hz in agreement with previous work on gold nanoparticles.[11,12] The characteristic bent at the corner frequency, known from typical tweezer power spectra, is not seen because the corner frequency is higher than the Nyquist frequency of the detection. Below 10 Hz the power spectral density is dominated by mechanical noise, for instance, drift. In addition, two noise peaks were always present at 94.14 Hz and 100 Hz.

Now turning on the chopped green scattering laser beam a significant peak is seen at the chopping frequency as well as at odd harmonics (Figure 3(b)). Note that the first noise peak in Figure 3(a) does not overlap the third harmonic of the chopping frequency. Zooms into a more narrow frequency range presented in Figures 3(c) and 3(d) reveal that the chopping frequency is very sharp. Since the force constant is known from the calibration measurement, the first order peak corresponding to the chopping frequency, $t_p^{-1} = 31.25$ Hz, can be used to determine the magnitude of the scattering force using Equation (3). With this, the data presented in Figure 3(b) reveal a measured scattering force of 23 fN. If the averaging technique demonstrated in Figure 2(b) is used, an average displacement $\Delta x = 6.6 \pm 0.9$ nm is found providing a scattering force of $F_S = \kappa \Delta x = 16 \pm 4$ fN. This corresponds well with the value found by power spectral density analysis.

In contrast to previous studies,[23,24] our experimental approach allows for applying post-elimination of thermal noise by averaging.[19] This significantly improves the resolution because due to application of a lock-in strategy, it is no longer limited by the standard deviation of the position

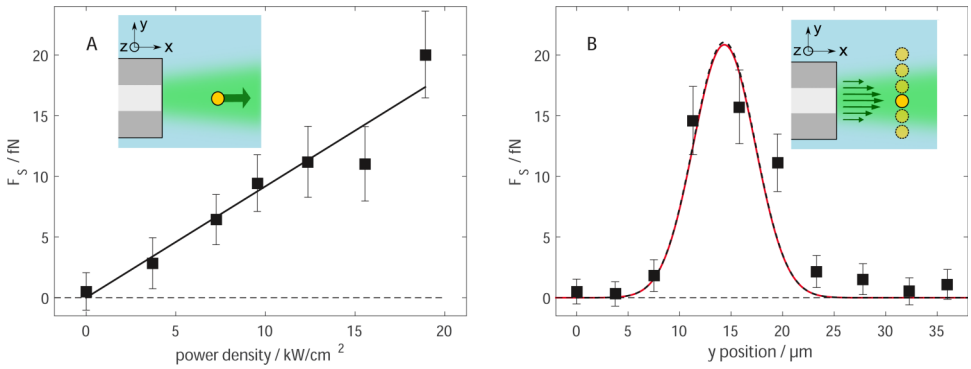

FIG. 4. (a) Measured scattering force versus applied output power of resonant laser light for $N = 2^{10}$ force pulses repeating with a frequency of 31.25 Hz corresponding to 32.77 s measurement time and (b) measurement of the scattering force for a spatial displacement along the Gaussian profile of the scattering beam for $N = 2^{11}$. In (a) and (b), the insetted plots are a sketch of the experimental configuration. Solid squares marks measured forces. The error bars correspond to a maximum error estimation. The red curve in (b) is the theoretical curve based on Mie simulations. Its width matches the full width half-maximum value of 8.0 ± 1.8 μm the Gaussian fit of the measured data (black dashed curve).

distribution, σ. It is rather limited by the averaged standard deviation, $\sigma_{avg} = \frac{\sigma}{\sqrt{N}}$, with $N = \frac{t_m}{t_p}$, the number of repetitions. The averaged standard deviation corresponds to averaged position data like the one shown in Figure 2(c) and provides for $N = 2^{11}$ a minimal force sensitivity of

$$\Delta F = \sigma_{avg}\kappa = \sqrt{\frac{k_B T \kappa}{N}} \approx 2.2 \text{ fN}$$

exploiting the relation of κ and σ via equipartition theorem.

Having characterized the system allows us to test whether the scattering force scales linearly with the power of the scattering beam. A series of measurement was done on a single particle kept at the same position. For each measurement we changed the power and measured 2^{10} chopping events. In Figure 4(a), solid squares correspond to a measured value of the scattering force. The errorbars of the plot are based on a maximum error calculation,[25] taking into account statistical uncertainties of the measured signal, the trap stiffness κ, deviation in the particle size r, and uncertainties in the temperature, T. The relative contributions of all quantities is of comparable magnitude. The values for the optical scattering force are in the low femtonewton regime and show a linear relationship to a power increase.

In order to test the spatial variation across the scattering beam, the position perpendicular to the beam direction was varied by moving the fiber relative to the trap. The resulting measured scattering forces are plotted in Figure 4(b). As expected, based on the Gaussian beam shape, the data points can be fitted with a Gaussian curve matching the beam width measured independently as described earlier. The maximal scattering force predicted from the fit of the spatial variation is $F_S^{exp} = 21.1$ fN. The error for the maximum measured force was 3.0 fN.

We can now compare the experimentally observed scattering force to theoretical calculations of force. A number of different approaches exist,[14,36,37] all relying on the dielectric function of single gold nanoparticles. The scientific community mostly agrees on the dielectric function for bulk gold provided by Johnson and Christy[38] in 1972. Their values are also chosen here. However, it should be mentioned that large deviations in the dielectric function have been reported by several different studies.[39,40] All these studies have been done for bulk gold, not for single particles. The choice of the refractive index of gold, and thus the dielectric function of gold, cause variations of up to 40% in the theoretically calculated values of the scattering force (see Figure S2 of the supplementary material[25]). This huge value spread reflects the difficulty of predicting optical scattering forces theoretically. Therefore, finding experimental methods like the one presented here is crucial in predicting and understanding optical scattering forces.

We performed calculations of the optical scattering force using an adapted version of the optical tweezers computational toolbox published by Nieminen *et al.*,[41] see the supplementary material

for details.[25] The results of the simulation with the parameters of the spatial variation experiment are compared with that measurement in Fig. 4(b). It is seen that the spatial dependency of the theoretical scattering force is a Gaussian curve with a maximum of $F_S^{theo} = 21.1$ fN (solid red curve). The maximum scattering force of the fit of the measured spatial variation is 21.1 ± 5.8 fN which is in excellent agreement with the theoretical prediction assuming a refractive index of gold as reported by Johnson and Christie[38] (see also supplementary material,[25] Figure S2 for a comparison with other values reported in the literature).

In conclusion we experimentally determined the scattering force acting on a single gold nanoparticle using optomechanical manipulation in combination with optical tweezers. Scattering forces were measured between 3 fN and 21 fN. This ultra-high sensitivity was enabled by using a quasi-lock-in technique that is based on repetitive pushing of an optically trapped gold nanoparticle followed by an analysis of the particle trace in both time and frequency domain. Applying this technique to a spatially varying scattering force field, we verified experimentally the Gaussian shape and magnitude predicted by theory. The experimental measurement of scattering forces on nanostructures with a method as proposed here can provide a more quantitative understanding of optomechanical manipulation experiments on the nanoscale.

Financial support by the SFB 1032, Project A8, is gratefully acknowledged. We would also like to thank Professor Jochen Feldmann for fruitful discussions.

[1] T. Hänsch and A. L. Schawlow, Opt. Commun. **13**, 68 (1975).
[2] T. J. Kippenberg and K. J. Vahala, Science **321**, 1172 (2008).
[3] K. C. Neuman and A. Nagy, Nat. Meth. **5**, 491 (2008).
[4] L. P. Ghislain, N. A. Switz, and W. W. Webb, Rev. Sci. Instrum. **65**, 2762 (1994).
[5] O. M. Marago, P. H. Jones, P. G. Gucciardi, G. Volpe, and A. C. Ferrari, Nat. Nanotechnol. **8**, 807 (2013).
[6] A. S. Urban, S. Carretero-Palacios, A. A. Lutich, T. Lohmüller, J. Feldmann, and F. Jäckel, Nanoscale **6**, 4458 (2014).
[7] A. Lehmuskero, P. Johansson, H. Rubinsztein-Dunlop, L. Tong, and M. Käll, ACS Nano **9**, 3453 (2015).
[8] S. Lal, S. Link, and N. J. Halas, Nat. Photonics **1**, 641 (2007).
[9] J. R. Moffitt, Y. R. Chemla, S. B. Smith, and C. Bustamante, Annu. Rev. Biochem. **77**, 205 (2008).
[10] K. Svoboda and S. M. Block, Opt. Lett. **19**, 930 (1994).
[11] P. M. Hansen, V. K. Bhatia, N. Harrit, and L. Oddershede, Nano Lett. **5**, 1937 (2005).
[12] F. Hajizadeh and S. S.Reihani, Opt. Express **18**, 551 (2010).
[13] A. Ohlinger, A. Deak, A. A. Lutich, and J. Feldmann, Phys. Rev. Lett. **108**, 018101 (2012).
[14] A. Rohrbach and E. H. K. Stelzer, J. Opt. Soc. Am. A **18**, 839 (2001).
[15] M. Dienerowitz, M. Mazilu, and K. Dholakia, J. Nanophotonics **2**, 021875 (2008).
[16] A. Ashkin, Phys. Rev. Lett. **24**, 156 (1970).
[17] G. Gouesbet, J. Quant. Spectrosc. Radiat. Transfer **110**, 1223 (2009).
[18] S. Eustis and M. A. El-Sayed, Chem. Soc. Rev. **35**, 209 (2006).
[19] T. B. Lindballe, M. V. G. Kristensen, K. Berg-Sørensen, S. R. Keiding, and H. Stapelfeldt, Opt. Express **21**, 1986 (2013).
[20] N. Villadsen, D. Ø. Andreasen, J. Hagelskjær, J. Thøgersen, A. Imparato, and S. R. Keiding, Opt. Express **23**, 13141 (2015).
[21] M. R. Pollard, S. W. Botchway, B. Chichkov, E. Freeman, R. N. J. Halsall, D. W. K. Jenkins, I. Loader, A. Ovsianikov, A. W. Parker, R. Stevens *et al.*, New J. Phys. **12**, 113056 (2010).
[22] D. B. Phillips, G. M. Gibson, R. Bowman, M. J. Padgett, S. Hanna, D. M. Carberry, M. J. Miles, and S. H. Simpson, Opt. Express **20**, 29679 (2012).
[23] O. M. Marago, P. H. Jones, F. Bonaccorso, V. Scardaci, P. G. Gucciardi, A. G. Rozhin, and A. C. Ferrari, Nano Lett. **8**, 3211 (2008).
[24] A. Rohrbach, Opt. Express **13**, 9695 (2005).
[25] See supplementary material at http://dx.doi.org/10.1063/1.4945351 for a derivation of Equation (3), the results of optical heating simulations for the particle surface temperature, and details on the error bar calculation for Figure 4 and the theoretical scattering force calculation.
[26] G. Falasco, M. V. Gnann, D. Rings, and K. Kroy, Phys. Rev. E **90** (2014).
[27] R. Parthasarathy, Nat. Meth. **9**, 724 (2012).
[28] M. Toshimitsu, Y. Matsumura, T. Shoji, N. Kitamura, M. Takase, K. Murakoshi, H. Yamauchi, S. Ito, H. Miyasaka, A. Nobuhiro *et al.*, J. Phys. Chem. C **116**, 14610 (2012).
[29] M. Perner, P. Bost, U. Lemmer, G. von Plessen, J. Feldmann, U. Becker, M. Mennig, M. Schmitt, and H. Schmidt, Phys. Rev. Lett. **78**, 2192 (1997).
[30] M. Hu and G. V. Hartland, J. Phys. Chem. B **106**, 7029 (2002).
[31] M. Fedoruk, M. Meixner, S. Carretero-Palacios, T. Lohmüller, and J. Feldmann, ACS Nano **7**, 7648 (2013).
[32] G. E. Uhlenbeck and L. S. Ornstein, Phys. Rev. **36**, 823 (1930).
[33] K. Berg-Sørensen and H. Flyvbjerg, Rev. Sci. Instrum. **75**, 594 (2004).
[34] W. P. Wong and K. Halvorsen, Opt. Express **14**, 12517 (2006).
[35] Release on the IAPWS Formulation 2008 for the Viscosity of Ordinary Water Substance, available online under http://www.viscopedia.com/viscosity-tables (02/2016) (2008).

[36] M. Mansuripur, Opt. Express **12**, 5375 (2004).
[37] J. P. Barton, D. R. Alexander, and S. A. Schaub, J. Appl. Phys. **66**, 4594 (1989).
[38] P. B. Johnson and R. W. Christy, Phys. Rev. B **6**, 4370 (1972).
[39] S. Babar and J. H. Weaver, Appl. Opt. **54**, 477 (2015).
[40] R. L. Olmon, B. Slovick, T. W. Johnson, D. Shelton, S.-H. Oh, G. D. Boreman, and M. B. Raschke, Phys. Rev. B **86**, 235147 (2012).
[41] T. A. Nieminen, V. L. Y. Loke, A. B. Stilgoe, G. Knoener, A. M. Branczyk, N. R. Heckenberg, and H. Rubinsztein-Dunlop, J. Opt. A: Pure Appl. Opt. **9**, S196 (2007).